

# Epicycles

William F. Barnes

April 20, 2022

# Contents

<b>1</b>	<b>Epicycles</b>	<b>2</b>
1	Introduction . . . . .	2
1.1	Ismail Al-Jazari . . . . .	2
1.2	Antikythera Mechanism . . . . .	3
1.3	Archimedes . . . . .	3
2	Universe of Ptolemy . . . . .	5
2.1	Ptolemaic System . . . . .	5
2.2	Planetary Symbols . . . . .	5
2.3	Retrograde Motion . . . . .	7
2.4	Epicycles . . . . .	7
2.5	Remarks . . . . .	8
3	Epicycle Clock . . . . .	10
3.1	Standard Clock . . . . .	10
3.2	Epicycle Clock . . . . .	10
3.3	Non-Twelve Hour Clocks . . . . .	11
3.4	Sidereal Time . . . . .	11
4	Drawing Continua . . . . .	14
4.1	Index Notation . . . . .	14
4.2	Horizontal Lines . . . . .	14
4.3	Arbitrary Straight Lines . . . . .	14
4.4	Ellipses . . . . .	15
4.5	Stars . . . . .	16
4.6	Lissajous Curves . . . . .	16
5	Connecting Discrete Points . . . . .	21
5.1	The Frequency Trick . . . . .	21
5.2	Squares . . . . .	23
6	Drawing Arbitrary Curves . . . . .	25
6.1	Motivation for DFT . . . . .	25
6.2	Complex Epicycles . . . . .	26
6.3	Discrete Fourier Transform . . . . .	27
6.4	Kronecker Delta Relations . . . . .	29
6.5	Implementing the DFT . . . . .	30
6.6	Open Curves . . . . .	31

# Chapter 1

# Epicycles

## Abstract

A method for plotting a curve through a sequence of points in the plane is developed. Curves are approximated by the sum of circular arcs called epicycles. Tracing a curve with epicycles entails calculating the Discrete Fourier Transform of original points.

## 1 Introduction

Humankind has been fascinated by idea of the *circle* for centuries. The cliche ‘invention of the wheel’, originating *somewhere* in Europe or China, or any point in between - nobody knows for sure - sparks the image of rolling transportation as the first useful implementation of the circle. Equally unclear is precisely where and when circles were first used for grinding tools, milling equipment, architecture, writing systems - the list goes on and on. In any case, most cultures seem to independently discover the ‘circle’ for themselves and put it to various uses.

### 1.1 Ismail Al-Jazari

An abstraction of the wheel, namely the *cogwheel*, or the *gear*, is at the center of virtually every invention since the eighteenth century. Before then, the first conceptualization of using cogwheels in machines is credited to Arab engineer Ismail Al-Jazari, whose career peaked around the year 1206.

Quite ahead of his time, Al-Jazari mastered a cross section of what we’d now call Newtonian mechanics, namely the ideas of leverage, mechanical advantage, gear ratios, and hydrostatics to name a few. Fig. 1.1 shows one of Al-Jazari’s devices depicted in his book, *The Book of Knowledge of Ingenious Mechanical Devices*. From his works, Al-Jazari clearly understood why inter-moving wheels can give rise to complex and precise outputs in a given machine.

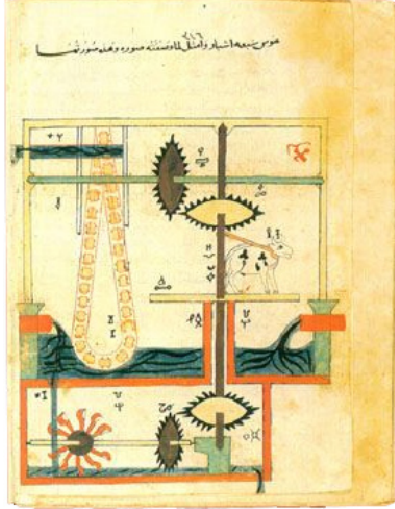


Figure 1.1: Hydro powered saqiya chain pump device illustrated in Al-Jazari’s *The Book of Knowledge of Ingenious Mechanical Devices*, 1206.



Figure 1.2: Antikythera mechanism photo released by the National Archaeological Museum in Athens, 2005.

## 1.2 Antikythera Mechanism

As if Al-Jazari wasn’t a historical enigma, leave it to the ancient Greeks to destroy all ancient stereotypes. A ship that sank sometime around 200 B.C. was carrying something now known as the *Antikythera mechanism*, depicted in Fig. 1.2, named after a neighboring island. The Antikythera mechanism is nothing short of a full-blown *analog computer* based on connected cogwheels that ‘calculates’ the goings of the Sun, Moon, and other celestial objects of ancient Greek astronomy. At least a thousand years ahead of its time, and more complex than a wristwatch, the Antikythera mechanism demonstrates the Greeks’ mastery of the wheel not just for easing repetitive farming tasks, but for handling *information* in mechanical form.

## 1.3 Archimedes

Suspiciously contemporary (or nearly so) to the Antikythera mechanism was the career of Archimedes, famous Greek mathematician and inventor. With regard to circles, ancient philosophers were already aware the circumference of a circle relates to its diameter in a fixed ratio, but Archimedes was the first to actually calculate this ratio rigorously, naming his result  $\pi$ .

While it is unclear whether Archimedes had anything to do with the Antikythera mechanism, it’s undeniable that the idea of ‘the circle’ was of enormous technical and theoretical interest to Greek intellectuals. It wouldn’t be long be-

fore the circle was hailed as the ‘divine’ shape. This idea spread, perhaps too thoroughly, all through the elementary sciences used by the Greeks.

## 2 Universe of Ptolemy

Simultaneous to the mechanical and mathematical achievements of the ancient Greeks were efforts to crack the problems of astronomy and cosmology. Unlike today, the ancients didn't (rather, couldn't) differentiate the workings of the local solar system from the grand clockwork of the Universe. To the Greeks, the Earth was the center of *all* things, and every motion in the night sky was set for the sake of Earthly drama. This, of course, is known as the *geocentric model* of the universe.

### 2.1 Ptolemaic System

Seeking an explanation for the apparent ‘perfect’ motions observed in the heavens, Greek philosopher Ptolemy (A.D 127-145) continued the assumption that the Earth remain fixed in space as the center of the universe. Then, measuring up from the ground, he supposed that the known celestial bodies - Moon, Mercury, Venus, Sun, Mars, Jupiter, Saturn - in that order, each moved on its own sphere concentrically surrounding the Earth. Depicted in Fig. 1.3 is an adaptation of the Ptolemaic model as ‘perfected’ for theological purposes.

As a refinement of the geocentric model, Ptolemy’s ‘concentric spheres’ model also takes care of the stars: since the stars in the night sky appear fixed relative to each other, Ptolemy reasoned the stars to all be embedded the same outermost sphere with Earth still at the center. This notion is still in use today, known by modern astronomers as the so-called *celestial sphere*.

Ancient astronomers also knew the apparent arc of a celestial object’s motion can be deduced over time by measuring its position at the same moment each night against the background of fixed stars. This is undoubtedly how the first few planets were discovered, and leads to why the standard year is partitioned into *months*, corresponding to the rough 30-day period of the Moon. The Sun is no exception to this pattern, for its motion too is apparently circular against the background of fixed stars, centered on Earth.

### 2.2 Planetary Symbols

Also evident in Fig. 1.3 are the ‘modern’ astronomical symbols used for the celestial bodies. For completeness, these are:

$\mathbb{C}$	= Moon
$\mathbb{M}$	= Mercury
$\mathbb{V}$	= Venus
$\odot$	= Sun
$\mathbb{M}$	= Mars
$\mathbb{J}$	= Jupiter
$\mathbb{S}$	= Saturn

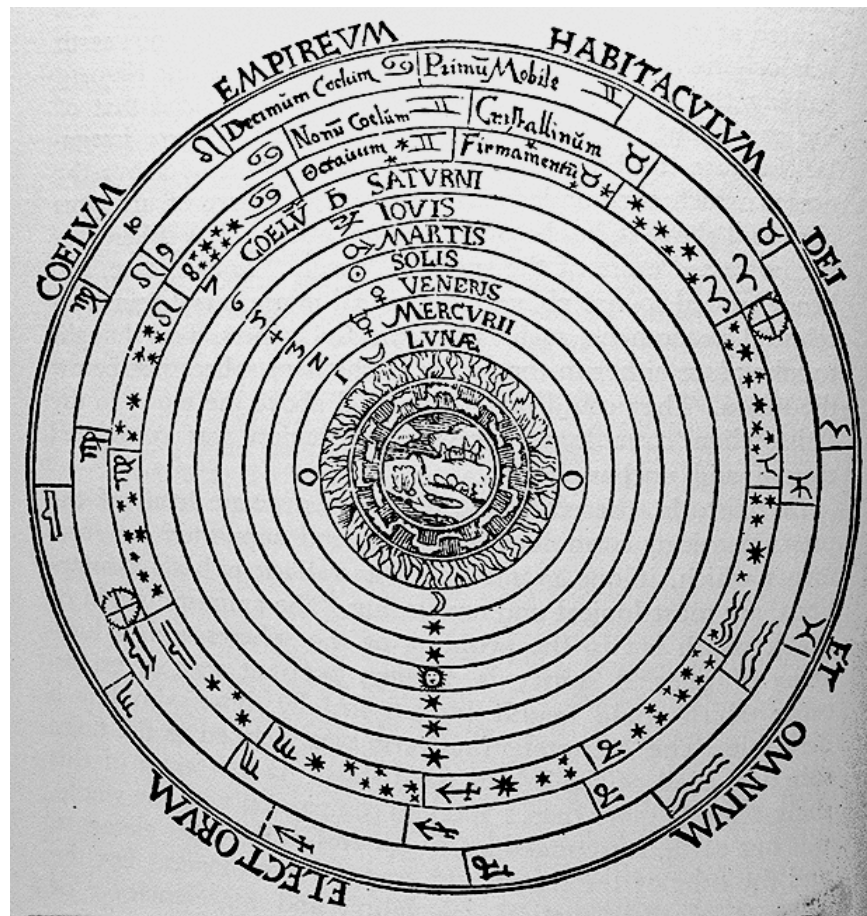


Figure 1.3: Engraving from Peter Apian's *Cosmographia*, depicting the *Christian Aristotelian cosmos*, 1524.

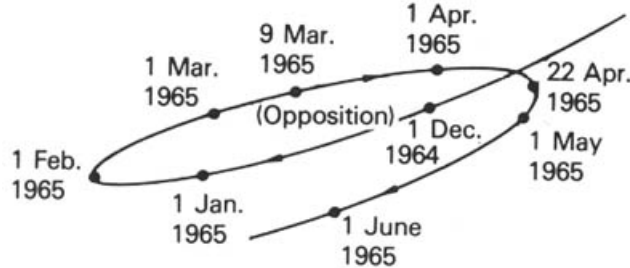


Figure 1.4: Retrograde motion of Mars. Originally in the *Book of Mars*, NASA SP-179 (1968).

Interestingly, the symbol for the Sun includes a ‘dot’, which is to denote the existence of *sunspots*, a well-known solar phenomena.

### 2.3 Retrograde Motion

The ‘measure-each-night’ trick does not work out so beautifully for planets, with Mars being a particularly striking example. Every two or so years, Mars seems to deviate from its proper arc as seen from Earth. Strangely, Mars goes *backward* against the night sky for several months, and then course-corrects to resume its normal path, completing a kind of figure-eight, or Z-like curve. The apparent backtracking of Mars, also exhibited by the other planets, became known as *retrograde motion*.

Since the original data used by Ptolemy isn’t forthcoming, we can use present-day data to approximate the view shared by the ancient Greeks. Depicted in Fig. 1.4 is the retrograde motion of Mars from Winter 1964 to Summer 1965 as seen from Earth by NASA. Faced with a similar observation, Ptolemy knew that retrograde motion would be the bitter end for a sphere-based model of the cosmos, but this just *couldn’t* be the case, because circles are supposed to be ‘perfect’. It would have been considered barbaric to propose new orbital shapes, such as ellipses, or to introduce any new element beside the circle. Ptolemy insisted that it be circles all the way down.

### 2.4 Epicycles

To wiggle his way out of the retrograde motion problem, Ptolemy supposed that Mars may not be ‘locked in place’ on its respective concentric sphere, but perhaps Mars also moves along a smaller circle embedded on the greater circle. The ‘smaller circle’ is called an *epicycle*, and the ‘greater circle’ is called the *deferent*. It turns out that adding epicycles to the geocentric model is the perfect ingredient to account for all celestial motions, including retrograde motion of the known planets. This refinement to the geocentric theory became known as the *Ptolemaic model*.

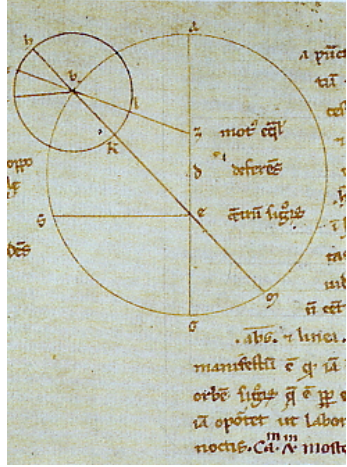


Figure 1.5: Claude Ptolemy, *Almagestum*, translated into Latin by Gerard of Cremona, 13th century. Vatican, Biblioteca Apostolica Vaticana, Lat. 2057.

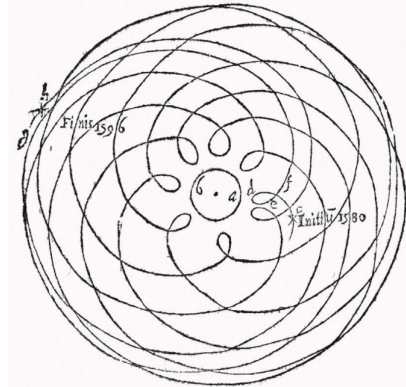


Figure 1.6: Epicycles of Mars as observed from Earth between 1580 and 1596. From *Sphaera mundi* (1635) by Italian astronomer Giuseppe Biancani (1566-1624). Released by Middle Temple Library (2016).

Shown in Fig. 1.5 is an ‘early’ reproduction of Ptolemy’s work on epicycles, published in the *Almagest*, published in roughly 150 A.D. Inspired by the Greeks, many astronomers took the Ptolemaic model as a starting point to work out the epicycle-based motions of Mars, Mercury, and so on for themselves. Fig. 1.6 depicts one such study that tracks the evident position of Mars over a sixteen-year interval.

The Ptolemaic model also took the interest of Arab astronomer Ibn al-Shatir (1304-1375). Working in a looser spirit than the Greeks, Ibn al-Shatir wasn’t so worried about the divinity of circles, and freely added an extra epicycle called the *Tusi-couple*, simplifying the theory. Depicted in Fig. 1.7 is Shatir’s explanation of the orbit of Mercury using epicycles. Among achievements similar to this, his works were collected in *kitab nihayat as-sul fi tashih al-usul*, retranslating to ‘A Final Inquiry Concerning the Rectification of Planetary Theory’.

## 2.5 Remarks

To garnish the Greek’s new-found the ability to account for celestial motions, epicycles were the affirmation that the circle really *is* the divine shape at the heart of cosmic motion. Ironically, this ‘circle bias’ drilled a little too deeply into the ancient worldview, and would eventually act to hinder progress in astronomy and other pursuits. The Ptolemaic model wouldn’t be successfully challenged - and only barely so - until the days of Copernicus (1543) and Galileo (1610), who dared to suggest that the Sun was the center of the solar system.

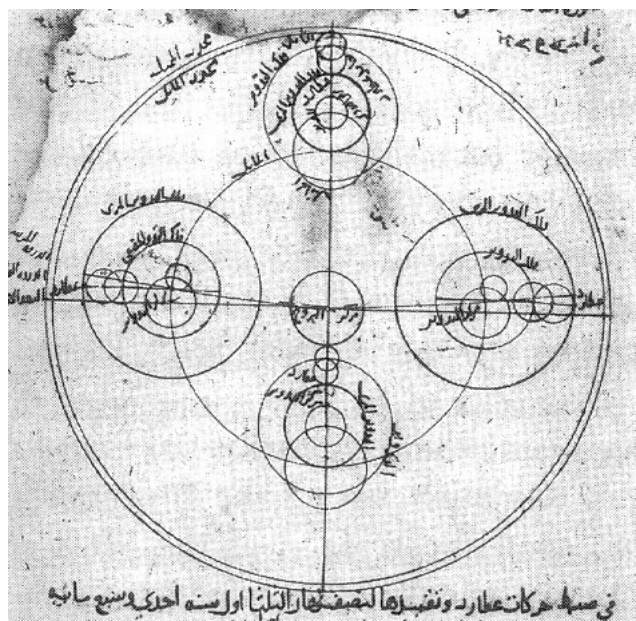


Figure 1.7: Ibn al-Shatir's explanation of the orbit of Mercury using epicycles.  
Wikimedia Commons.

### 3 Epicycle Clock

Taking a 21st-century view of epicycles, it's been clear since the days of Newton (1642-1727) that circles are *not* the key to understanding orbits in the solar system. This does not mean, however, that epicycles should be condemned to a dusty shelf as a triviality. It turns out that the reasoning behind epicycles requires a tour of duty through early college-level mathematics, which is to mean one must be somewhat comfortable with trigonometry, vectors, and parameterized motion at the outset. To quickly review these, let us take a small delve into epicycles to build a toy analog clock.

#### 3.1 Standard Clock

Imagine a standard analog clock with the usual ‘hour’, ‘minute’, and ‘second’ hands. Placing the origin of a Cartesian system at the center of the clock face, the ‘tip’ of the hour hand can be written as a vector:

$$\vec{H} = \langle R_H \cos(\theta_H), R_H \sin(\theta_H) \rangle$$

In the above,  $R_H$  is the length of the hour hand, and the variable  $\theta_H$  is an angular parameter that represents each hour and all moments in between. By convention  $\theta = 0$  corresponds to 3:00, and  $\theta_H$  increases in the *counterclockwise* direction, if that weren't confusing enough. This means  $\pi/2$  corresponds to 12:00,  $\pi$  corresponds to 9:00, and so on.

On a standard clock, the minute hand and second hands are also pinned to the origin, having respective vector representations:

$$\begin{aligned}\vec{M} &= \langle R_M \cos(\theta_M), R_M \sin(\theta_M) \rangle \\ \vec{S} &= \langle R_S \cos(\theta_S), R_S \sin(\theta_S) \rangle\end{aligned}$$

To be more precise, each angular parameter  $\theta_j$  is a function of time, equal to

$$\theta_j(t) = -\omega_j t + \phi_j \quad j = H, M, S,$$

where the angular velocity of each hand is captured by  $\omega_j$ , and  $t$  is the time parameter. The phase  $\phi_j$  is tuned at  $\pi/2$  so all clock hands overlap at 12:00 when  $t = 0$ . The way we capture one hour having 60 minutes, and one minute having 60 seconds, is by restricting the angular velocities:

$$\omega_S = 60 \omega_M = 60 (60 \omega_H)$$

#### 3.2 Epicycle Clock

Now let us modify the analog clock to be more epicycle-like. The hour hand shall be based at the origin as before. As for the minute hand, we choose its base as the tip of the hour hand. Similarly, the second hand is placed at the tip of the minute hand. All together, this means that the ‘time vector’

$$\vec{T}(t) = \vec{H}(t) + \vec{M}(t) + \vec{S}(t)$$

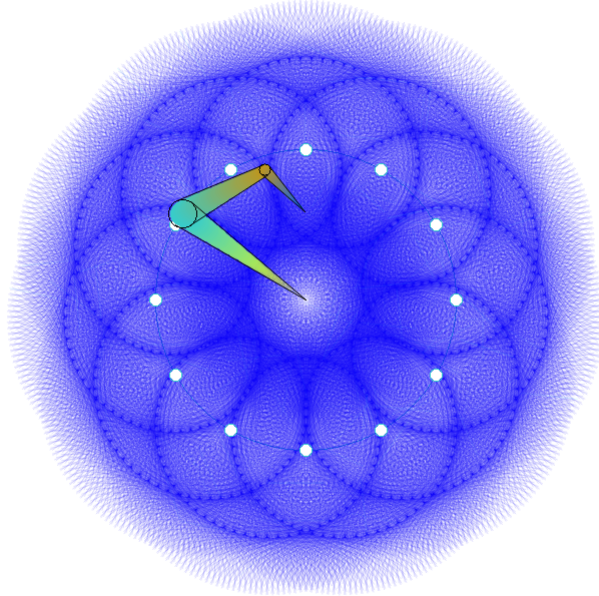


Figure 1.8: Twelve-hour epicycle clock displaying time 10:10:23.

lands at a specific place in the Cartesian plane for each value of  $t$ .

Shown in Fig. 1.8 is such a clock displaying the time 10:10:23. The shaded backdrop image is comprised of  $60 \times 60 \times 60$  total lines, generated by tracing the second hand once for all possible times. As the clock runs, the hour hand traces out its ‘usual’ circle. The minute hand though, because it’s not pinned to the center, must swing around the hour hand, and likewise for the second hand. For this reason, we call this scheme the *epicycle clock*.

### 3.3 Non-Twelve Hour Clocks

An interesting modification to the epicycle clock changes the total period from 12 hours to some other number. This isn’t to say the hour, minute, or second are redefined - only the ‘reset time’ of the clock. Shown in Fig. 1.9 is a *six-hour* clock displaying the time 04:21:21. Note that minute and second hands still occupy values from 0 to 60 to complete a revolution. It also follows that when the ‘minutes’ and ‘seconds’ are the same number, the hands become momentarily parallel as shown.

### 3.4 Sidereal Time

One interesting detail of the epicycle clock is that the number of complete ‘loops’ traced out by the minute hand is *one less* than the number of hours on the clock. For instance, the minute hand completes 11 loops on the 12-hour

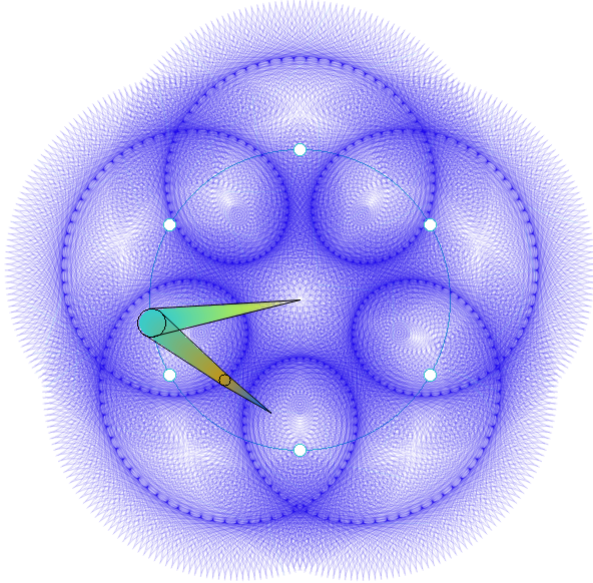


Figure 1.9: Six-hour epicycle clock displaying time 04:21:21. The minute- and second-hands are momentarily parallel when ‘minutes’ and ‘seconds’ are the same number.

clock. On the 6-hour clock, there are 5 loops. No matter how many hours are on the clock, there is always an ‘off-by-one’ discrepancy for the number of complete revolutions carried out by the minute hand.

Applying the same analysis to *modern* (heliocentric, Newtonian) planetary motion, particularly Earth, it’s possible to raise doubt about the number of days in one year. For a while now, we’ve agreed that there are about 365.2422 days in one year, but on *which* side of the off-by-one error is this number based on?

It turns out that modern astronomers have framed this problem by introducing *sidereal time* and *anit-sidereal time*. Consider the rotation of Earth *only*, ignoring the effect of going around the sun. Based on the apparent motion of the stars across the sky as measured from a fixed point on Earth, one would measure the ‘day’ to be not 24:00 hours (88512 seconds), but instead 23:56:04 (86164.0905 seconds). This time is called the *sidereal day*, i.e., the ‘pure’ rotation period of the Earth with respect to the fixed stars.

On the other hand, suppose instead that Earth did *not* rotate on its axis, but still revolves around the sun (ignoring the stars). In this situation, there is still a notion of sunrise and sunset on Earth, with a period of exactly one year. This effectively means that a complete year results a ‘free day’. It’s in this way that *solar time* is defined. Since the actual Earth rotates *and* revolves, and it’s convenient for Earthly affairs to base local clocks on the apparent solar time. The apparent solar time is of course modified by Earth’s angular velocity.

Summarizing these ideas, we must acknowledge that if Earth's year is precisely  $N$  days, only  $N - 1$  of those days correspond to rotation about the axis, and one day comes about by revolution around the Sun.

## 4 Drawing Continua

As we've seen, epicycles are naturally suited to sketching curves, usually closed, clover-like shapes with a fair degree of symmetry. It turns out that, with enough cleverness, epicycles can be used to trace many more families of curves, even arbitrary curves.

### 4.1 Index Notation

At any time  $t$ , the so-called ‘drawing tip’ in the epicycle construction is somewhere in the Cartesian plane. Using standard trigonometry, it's easily seen that the curve traced out by  $N$  epicycles is given by:

$$x(t) = \sum_{j=1}^N r_j \cos(\phi_i + \omega_j t)$$
$$y(t) = \sum_{j=1}^N r_j \sin(\phi_i + \omega_j t)$$

In the above,  $r_j$  is each radius,  $\omega_j$  is each angular frequency, and  $\phi_j$  is each initial phase. One sees that the initial phase  $\phi_1$  determines the orientation of a straight line, with  $\phi_1 = 0$  corresponding to the horizontal case. As we blaze through examples to get a feel for epicycle drawing, remember that *all* of the information is contained in the table:

$$\{r_j, \omega_j, \phi_j\} \quad j = 1, 2, 3, \dots, N$$

### 4.2 Horizontal Lines

Starting with one of the easiest cases first, straight lines through the origin are exceedingly simple to draw with circles. The recipe requires two epicycles having equal radius and equal-and-opposite rotation speeds. Visualizing this in steps, Fig. 1.10 shows the so-called *one-circle* approximation to a given horizontal straight line, where a line that swivels about the origin traces out a circle in the Cartesian plane. This clearly can't be the final answer, the circle only touches the line twice. Note too that this first-order circle goes clockwise for increasing time.

By introducing the next epicycle, and tracing a point on its rim, we come up with the *two-circle* approximation. It happens that this case perfectly produces a horizontal line, shown in Fig. 1.11. In the Figure, it's evident why each epicycle have equal radius but opposite rotation rates. In this case, a point on the rim of the second circle has a constant height.

### 4.3 Arbitrary Straight Lines

The family of epicycles must accommodate a circle that does *not* rotate, which amounts to interpreting  $r_0$  and  $\phi_0$  as an overall offset in the resulting curve.

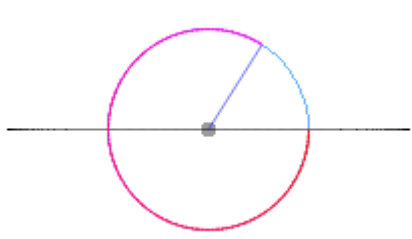


Figure 1.10: One-circle approximation of horizontal line, only correct at two points.

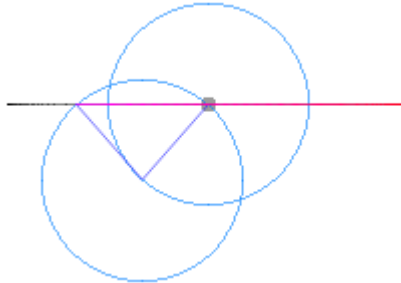


Figure 1.11: Two-circle approximation of horizontal line, correct at all points.

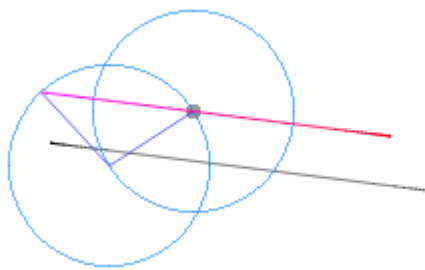


Figure 1.12: One-circle approximation of horizontal line, correct up to a constant offset.

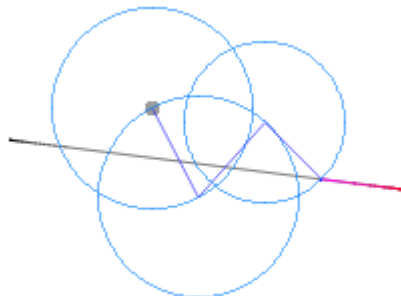


Figure 1.13: Two-circle approximation of horizontal line, corrected with a non-rotating epicycle.

Fig. 1.12 illustrates the order-two approximation of a straight line, but the line is clearly offset. We correct for this by choosing just the right  $r_0, \phi_0$  for a non-rotating base-zero epicycle, leading to Fig. 1.13.

With lines figured out, it is tempting to think that squares and rectangles are an open-and-shut case for epicycles. This isn't quite the case, as one can imagine that the abrupt 90-degree corners of a square require more than just a few orders of approximation to get right.

#### 4.4 Ellipses

By simply changing the radius of either used to generate a straight line, the resulting shape is elliptical. If the respective radii are  $r_1 > r_2$ , then the semi-major axis is the sum  $r_1 + r_2$ , and the semi-minor axis is the difference  $r_1 - r_2$ . Demonstrated in Fig. 1.14 is the case with  $r_1 = 2r_2$ .

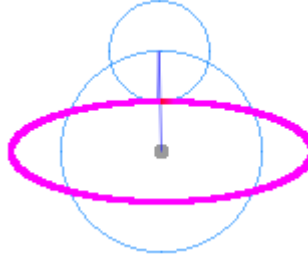


Figure 1.14: Tracing an ellipse using two circles of unequal radii and equal and opposite rotation rates.

## 4.5 Stars

A surprising ‘comfort zone’ for epicycles is the family of ‘stars’. To construct any given star, we choose a pair of counter-rotating circles with non-equal radii and non-equal rotation rates. Supposing one circle rotates at positive rate  $\omega_1$ , and the other has negative rate  $-\omega_2$ , the number of points in the resulting star is equal to  $\omega_1 - \omega_2$ .

Two example cases are detailed in Figs. 1.15, 1.16. The first case is generated with the following data:

$$\begin{aligned} r_j &= \{50, 25\} \\ \omega_j &= 2\pi \cdot \{2, -3\} \\ \phi_j &= \{-\pi, \pi/4\} \end{aligned}$$

Likewise, for the second case:

$$\begin{aligned} r_j &= \{50, 35\} \\ \omega_j &= 2\pi \cdot \{3, -4\} \\ \phi_j &= \{-\pi, \pi/4\} \end{aligned}$$

## 4.6 Lissajous Curves

### Cartesian Formulation

A *Lissajous curve*, also known as a Bowditch curve, is the image of the set of parametric equations:

$$x(t) = A \sin(2\pi at + \delta) \quad y(t) = B \sin(2\pi bt)$$

The constants  $A$  and  $B$  respectively control the horizontal and vertical scales. Inside the sine function, the constants  $a$  and  $b$  are angular frequencies, where  $\delta$ , conventionally associated with the  $x$ -equation, is an overall phase shift. The

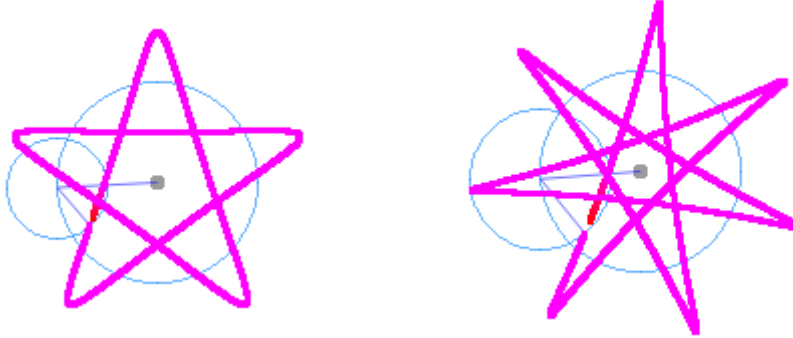


Figure 1.15: Five-vertex star plotted with two epicycles.

Figure 1.16: Seven-vertex star plotted with two epicycles.

ratio  $a/b$  determines the overall ‘fingerprint’ of the curve. A Lissajous curve is *closed* when  $a/b$  is rational.

With so many variables in play, it’s prudent to explore Lissajous curves by limiting  $A = B$ , and also restricting  $a, b$  to integer values. Plotted in Fig. 1.17 is a table of Lissajous curves for various choices of  $a, b$ , and  $\delta$ .

### Epicycle Formulation

Recall that a straight lines can be traced out using two epicycles of the same radius with equal-and-opposite rotation rates. The placement and orientation of any line is controlled by the initial phase of each epicycle involved, with a maximum of three.

To bump things up a notch, let us consider *two* pairs of counter-rolling epicycles instead of one pair, all with a common radius. Believe it or not, this is exactly the formula for Lissajous curves, as long as we get all of the angular frequencies and phases right.

To illustrate this, take a Lissajous curve such as any from Fig. 1.17. Choosing the curve with  $a = 3, b = 1, \delta = \pi + \pi/4$  for the sake of argument. (Note too that  $a, b$  are scaled by  $2\pi$ .) From this, we need an equivalent representation in the form

$$\{r_j, \omega_j, \phi_j\} \quad j = 1, 2, 3, 4,$$

where the zero-case can be ignored (the Lissajous curve is already centered). We also won’t worry much about the  $r_j$ -variable, for this is one and the same number across each  $j$ :

$$r = r_1 = r_2 = r_3 = r_4$$

With some fiddling, one can easily-enough work out the proper mapping from  $a, b, \delta$ , onto  $\omega_j, \phi_j$ . For our case, this turns out to be:

$$\omega_1 = b = -\omega_3 \quad \omega_2 = a = -\omega_4$$

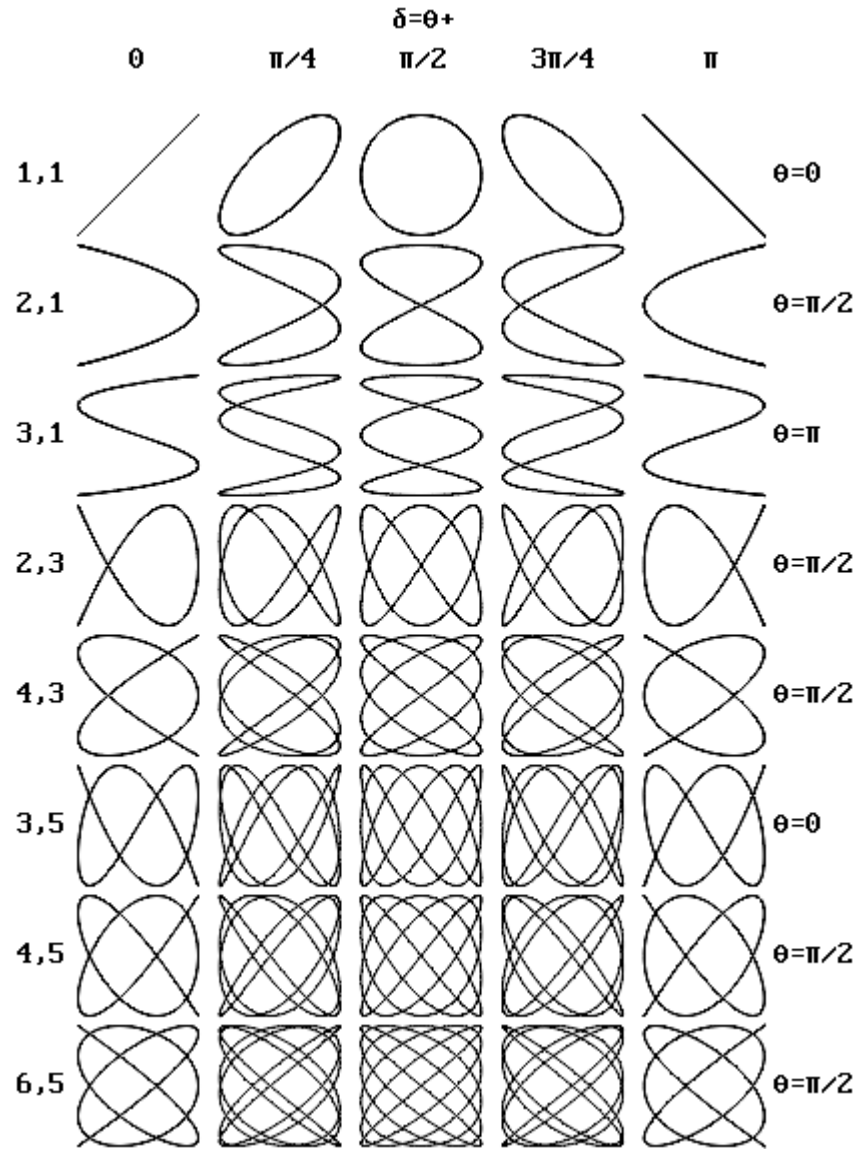


Figure 1.17: Table of Lissajous curves. Indexed vertically are respective angular frequencies  $a, b$  (scaled by  $2\pi$ ). The phase shift  $\delta$  is indexed horizontally.

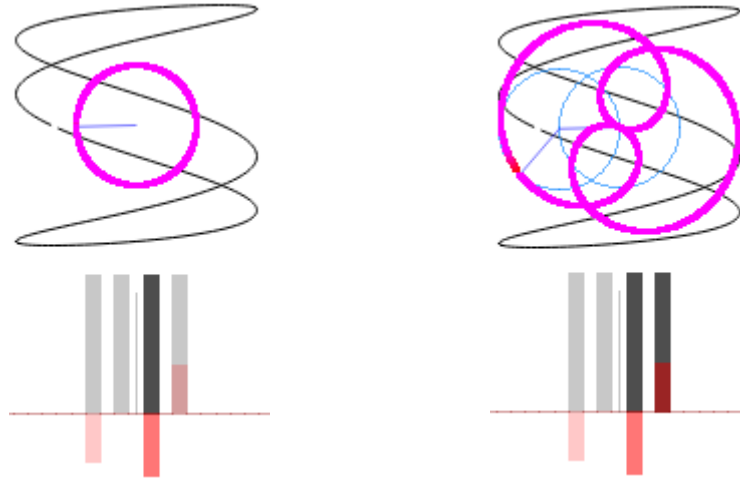


Figure 1.18: One-circle approximation of a Lissajous curve.

Figure 1.19: Two-circle approximation of a Lissajous curve.

$$\phi_j = \{-\pi, 3\pi/4, 0, -3\pi/4\}$$

Note that  $\omega_1$  is assigned to the lesser of the given angular frequencies, and  $\omega_2$  always takes the greater.

Having specified a given Lissajous curve in terms of epicycles, we can witness the the curve being gradually constructed. Staying with our running example, Figs. 1.18-1.21 illustrate increasing orders of approximatioon to the Lissajous curve, settling on fourth-order, giving the exact result. Positioned below each curve is a plot representing the radius (grey) and phase (red) of each epicycle used.

It turns out that any Lissajous curve from the family depicted in Fig. 1.17 can be generated by the same process demonstrated above. The angular frequencies  $a, b$  are straightforwardly assigned to each  $\omega_j$  as discussed, however the setting the initial phase  $\phi_j$  for each case can be quite a chore to do manually.

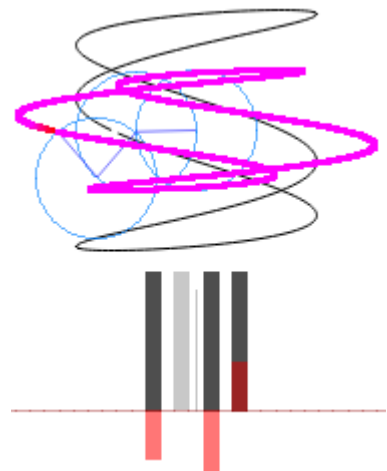


Figure 1.20: Three-circle approximation of a Lissajous curve.

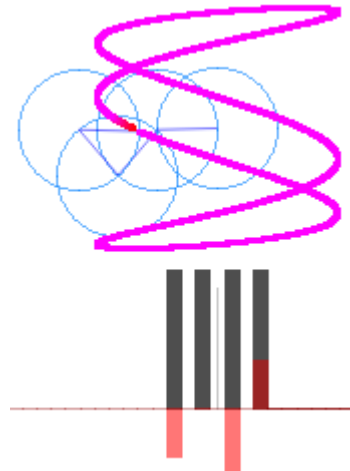


Figure 1.21: Four-circle (final) approximation of a Lissajous curve.

## 5 Connecting Discrete Points

### Resolution

Things become more interesting when we acknowledge that computers and plotting programs work in a paradigm of rigid bits rather than continua. To do meaningful work, it becomes necessary to recast continuous inputs and continuous outputs as sets of discrete packets in hopes that the end result appears ‘continuous enough’. The accuracy of a discrete-point approximation to a curve depends on the number of points being used, called the *resolution*. In the limit of infinite resolution, a discrete model blurs back into continuum.

‘Resolution’ in the context of epicycles refers to the number of circles  $N$  required to draw a smooth curve through  $P$  particular points in the plane. Since epicycles trace continuous arcs by definition, there will be more ‘curve on the page’ than would arise from a linear connect-the-dots approach. For  $N < P$ , the resulting curve attempts to trace out the shape implied by all  $P$  points, but is only ‘exact’ for the case  $N = P$ .

### 5.1 The Frequency Trick

Consider the ordered list of three points  $(-30, 15)$ ,  $(20, 65)$ , and  $(-20, -50)$ . With three points given, one immediately knows (at most) three epicycles are required to connect the points in order:

$$\{r_j, \omega_j, \phi_j\} \quad j = 1, 2, 3$$

In total, there are six known quantities - two for each point - however there are *nine* unknown quantities. This is three unknowns too many to specify a solution, so an additional insight is needed.

One eventually notices that the applicable  $\omega_j$  for small  $N$  should also be small, which is to say fast-rotating epicycles aren’t required to trace only three points. In fact, the *only* frequencies in play ought to be

$$\omega_j = 2\pi \cdot \{-1, 0, 1\} .$$

With the ‘frequency trick’ restriction on  $\omega_j$ , the epicycle representation for this problem can be written as a system with only six unknowns:

$$\{r_j, j, \phi_j\} \quad j = -1, 0, 1$$

How such a system is solved is slightly nontrivial, but at least we know there probably is a solution.

Leaving the details aside for now, it happens that the three points  $(-30, 15)$ ,  $(20, 65)$ , and  $(-20, -50)$  are approximated by:

$$\begin{aligned} r_j &= \{14.14, 45.42, 24.90\} \\ \omega_j &= 2\pi \cdot \{0, 1, -1\} \\ \phi_j &= \{-2.356, -2.827, 0.3719, \} \end{aligned}$$

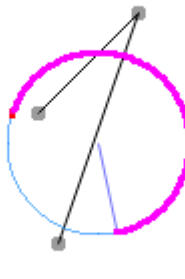


Figure 1.22: One-circle approximation of three given points using frequency number 1, ignoring  $-1, 0$ .

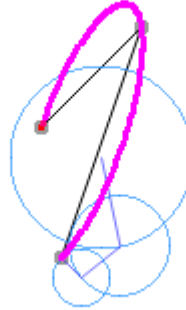


Figure 1.23: Three-circle approximation of three given points using frequency numbers  $-1, 0, 1$ .

Figs. 1.22, 1.23 show the respective one-circle and three-circle approximations of the three given points. As promised, there is more than enough curve to go around, and there is almost no telling what the curve will do when it's not passing through any of the  $P$  points.

### Generalized Frequency Trick

It should make sense that the so-called frequency trick works in general for  $2N + 1$  total points, in which case we tack on a new frequency number for each new point added:

$$\omega_j = 2\pi \cdot \{-N, \dots, -2, -1, 0, 1, 2, \dots, N\}$$

The case  $\omega_j = 0$  corresponds to the epicycle that does not rotate, but instead offsets the entire curve by a constant vector.

### Positive Frequencies Only?

It's worth wondering if  $N$  given points can be connected using epicycles with non-negative frequencies *only*. This is in fact possible, however the resulting curve is prone to throwing much more ‘ink on paper’ to achieve connecting all points. Shown in Fig. 1.24 is the result of using non-negative frequencies to connect the the same three points examined previously.

The positive-frequencies modification to seems harmless until we try it on more shapes, such as the Lissajous curve previously examined. Fig. 1.25 shows first few plotting cycles before the image is flooded with points. It's for this reason that the regime allowing negative  $\omega_j$  is preferred.

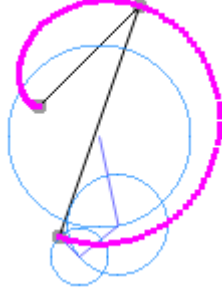


Figure 1.24: Three-circle approximation of three given points using non-negative frequency numbers 0, 1, 2.

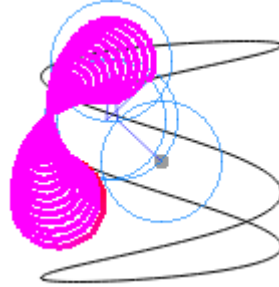


Figure 1.25: Four-circle approximation of Lissajous curve using non-negative frequency numbers.

## 5.2 Squares

Unlike lines, simple arcs, and Lissajous curves, it should follow that shapes featuring rigid corners and spikes don't follow a smooth parameterization. For this reason, it's necessary to approximate things like squares, particularly because of the corners, using more than just a few epicycles.

In effort to 'guess' the correct epicycle representation for a square, let's first assume the square is represented by  $P$  discrete points, and thus it requires  $N$  epicycles to trace through each point. Using the so-called frequency trick, the angular frequencies can safely be assumed as

$$\omega_j = 2\pi \cdot \{0, \pm 1, \pm 2, \dots\}.$$

Of course, not all frequencies may be present in the square's final approximation.

Seeking any guess for the radius values  $r_j$  and phase values  $\phi_j$ , begin with the observation that the *greatest* distance from the origin traced by an epicycle is any corner of the square. To reach the top-right corner, every phase must be momentarily in agreement, having value  $\phi_j = \pi/4$ . This occurs at three more instants, namely  $\phi_j = -\pi/4$  and  $\phi_j = \pm 3\pi/4$ . When all of the phases are in sync, the length of the epicycle 'drawing arm' is the sum of all  $r_j$ . If the total width of the square is  $2A$ , then we may write

$$A\sqrt{2} \approx \sum_{j=1}^N r_j.$$

By similar arguments, the *shortest* distance from the origin occurs at four points on the square, and we must have

$$A \approx \sum_{j=1}^N a_j r_j$$

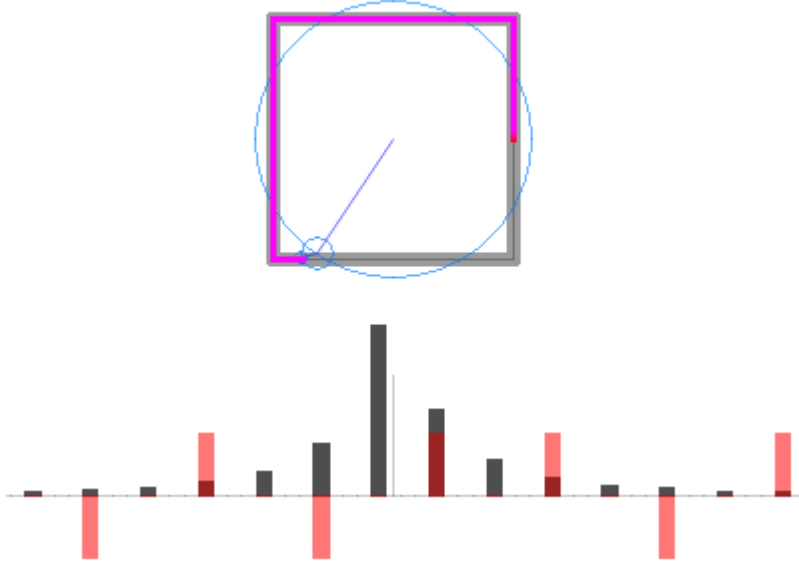


Figure 1.26: Approximation of a square based on  $N = 8000$  points. Under the curve in grey is  $\ln(1 + r_j)$  versus  $\omega_j$ , centered at  $\omega_0 = 0$ . The corresponding phase  $\pm\pi$  is superimposed in red.

for some set of coefficients  $\{a_j\}$ .

At this stage, we have two equations for  $r_j$  that are vaguely suggestive of  $\phi_j$ . Solving for  $r_j, \phi_j$  this way is a very hard problem, so let us (once again) leave certain details aside, and simply list the correct answer. Choosing  $A = 1$ , it turns out that, approximately:

$$\begin{aligned} r_j &= \{1.146, 0.1274, 0.04585, 0.02339, 0.01415, 0.009473, \dots\} \\ \omega_j &= \{-1, 3, -5, 7, -9, 11, -13, \dots\} \\ \phi_j &= \{0, \pi, -\pi, 0, 0, \pi, -\pi, 0, 0, \dots\} \end{aligned}$$

Reconciling this with the sums above, we can write

$$\begin{aligned} \sqrt{2} &\approx 1.146 + 0.1274 + 0.04585 + 0.02339 + 0.01415 + 0.009473 + \dots \\ 1 &\approx 1.146 - 0.1274 - 0.04585 + 0.02339 + 0.01415 - 0.009473 - \dots \end{aligned}$$

Fig. 1.26 illustrates the epicycle approximation of a square based on  $N = 8000$  points. Plotted under the curve in grey is  $\ln(1 + r_j)$  versus  $\omega_j$ , centered at  $\omega_0 = 0$ . The corresponding phase  $\pm\pi$  is superimposed in red. Interestingly, the sequence of  $r_j$  seems to stabilize around the values listed, with increased resolution  $N$  mattering little beyond  $N \approx 400$ .

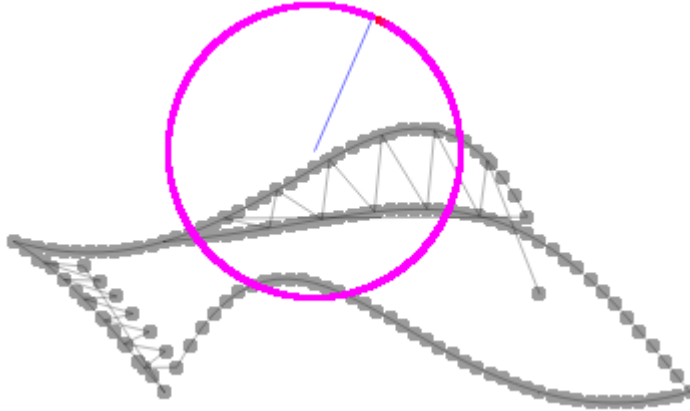


Figure 1.27: Vince’s fish, raw.

## 6 Drawing Arbitrary Curves

By now, it’s becoming evident that epicycles can be used to connect *any* sequence of points in the Cartesian plane. Using the generalized frequency trick, we can already stop worrying about  $\omega_j$  by writing

$$\omega_j = 2\pi \cdot \{0, \pm 1, \pm 2, \dots\} .$$

Then, the remaining job is to find all  $r_j$  and  $\phi_j$ , from  $P$  given points.

In case this seems impossible, or if you suspect at this moment that every example encountered has been too contrived, I present to you Vince’s fish, depicted in Figs. 1.27-1.28. The ‘uncooked’ fish consists of 168 ordered pairs. Using one epicycle per point, the final approximation to the fish is eerily accurate. The message is, it would be just about impossible to come up with the ‘cooked’ fish by manually fiddling around with  $r_j$  and  $\phi_j$ . There is, in fact, a fully general trick for calculating all  $r_j$  and  $\phi_j$  from  $P$  given points, called the *discrete Fourier transform*, or DFT for short.

### 6.1 Motivation for DFT

Consider a given ordered list of  $P$  ordered pairs  $(x, y)$  on the Cartesian plane:

$$\{x_p, y_p\} \quad p = 1, 2, 3, \dots, P$$

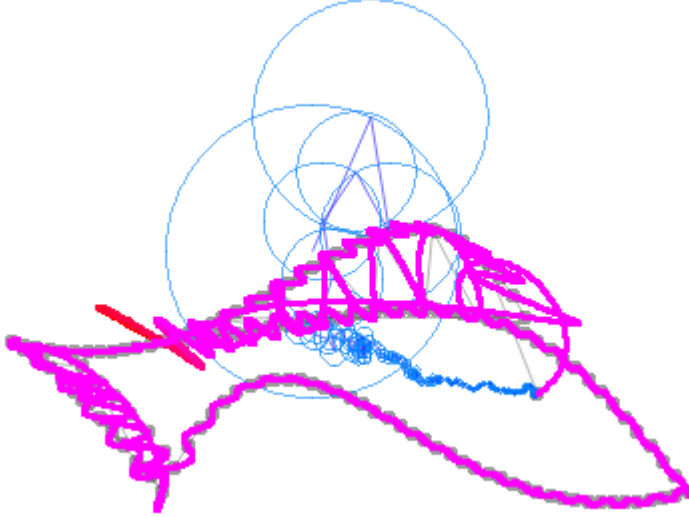


Figure 1.28: Vince’s fish approximated by 168 epicycles (fully cooked).

The task on hand is to represent the  $p$ th point somewhere on the perimeter of the  $N$ th epicycle:

$$x_p = \sum_{j=1}^{N \leq P} r_j \cos(\phi_i + \omega_j t_p) \quad (1.1)$$

$$y_p = \sum_{j=1}^{N \leq P} r_j \sin(\phi_i + \omega_j t_p) \quad (1.2)$$

Note that when  $N = P$ , the above equations are guaranteed to send the resulting curve directly through each point.

## 6.2 Complex Epicycles

With the polar representation of each  $x_p, y_p$ , it makes sense to combine these into a complex number such that

$$z_p = x_p + iy_p \quad (1.3)$$

for each  $p$ . Then (1.1), (1.2) join to become

$$z_p = \sum_{j=1}^N (r_j \cos(\phi_i + \omega_j t_p) + i r_j \sin(\phi_i + \omega_j t_p)) ,$$

which, by Euler's formula, is equivalent to:

$$z_p = \sum_{j=1}^N r_j e^{i\phi_j + i\omega_j t_p} \quad (1.4)$$

To get a grip on the time dependence, let us first associate each point  $p$  with a unique value on the interval  $[0 : 2\pi)$  such that

$$t_p = \frac{2\pi p}{N} \quad p = 0, 1, 2, \dots, N-1. \quad (1.5)$$

By doing so, the angular frequencies  $\omega_j$  become dimensionless integers:

$$\omega_j = j \quad j = 0, 1, 2, \dots, N-1 \quad (1.6)$$

You may trade factors like  $2\pi$  from the  $t_p$ -variable to the  $\omega_j$  variable without harm.

An equivalent but more convenient choice for the angular frequencies  $\omega_j$  allows for negative values:

$$\omega_j = \left\{ 0, \pm 1, \pm 2, \pm 3, \dots, \frac{N}{2} \right\}$$

To get this from (1.6), we write the conditional substitution:

$$\omega_j = \begin{cases} j & \text{if } j \leq N/2 \\ j - N & \text{if } j > N/2 \end{cases} \quad (1.7)$$

It also makes sense to separate time-dependent terms from the constant terms, so let's define a complex number  $Q_j$  such that

$$Q_j = r_j e^{i\phi_j}, \quad (1.8)$$

which combines the radius and the initial phase of each epicycle. Putting everything together, we so far have

$$z_p = \sum_{j=0}^{N-1} Q_j e^{i2\pi j p / N}. \quad (1.9)$$

### 6.3 Discrete Fourier Transform

The big job now is to solve (1.9) for each complex coefficient  $Q_j$ . This is done by a method called *Fourier's trick*, which begins by introducing a similar exponential term with a negative argument, particularly

$$e^{-i2\pi k p / N},$$

where the ‘frequency index’  $j$  is changed to  $k$ . Multiply this quantity into (1.9) and sum over  $p$ :

$$\begin{aligned} \sum_{p=0}^{N-1} z_p e^{-i2\pi kp/N} &= \sum_{p=0}^{N-1} \sum_{j=0}^{N-1} Q_j e^{i2\pi jp/N} e^{-i2\pi kp/N} \\ &= \sum_{j=0}^{N-1} Q_j \sum_{p=0}^{N-1} e^{i2\pi(j-k)p/N} \end{aligned}$$

It’s possible to prove (see below) that the right-most sum evaluates to a Kronecker delta relation

$$\sum_{p=0}^{N-1} e^{i2\pi(j-k)p/N} = N \delta(j - k),$$

and the above reduces to

$$\sum_{p=0}^{N-1} z_p e^{-i2\pi kp/N} = N \sum_{j=0}^{N-1} Q_j \delta(j - k) = N Q_k.$$

The effect of  $\delta(j - k)$  is to ‘pluck out’  $Q_k$  from the remaining sum, while flattening all other terms to zero. After realizing this, we have a formula for  $Q_j$  as it appears in (1.9):

$$Q_j = \frac{1}{N} \sum_{p=0}^{N-1} z_p e^{-i2\pi jp/N} \quad (1.10)$$

For a consistency check, it’s worth plugging (1.10) back into (1.9) to make sure  $z_p$  comes back out:

$$\begin{aligned} z_p &= \sum_{j=0}^{N-1} Q_j e^{i2\pi jp/N} = \sum_{j=0}^{N-1} \frac{1}{N} \sum_{p'=0}^{N-1} z_{p'} e^{-i2\pi jp'/N} e^{i2\pi jp/N} \\ &= \sum_{p'=0}^{N-1} z_{p'} \left( \frac{1}{N} \sum_{j=0}^{N-1} e^{i2\pi j(p-p')/N} \right) \\ &= \sum_{p'=0}^{N-1} z_{p'} \delta(p - p') = z_p \end{aligned}$$

Note that a similar Kronecker delta relation has been used.

## 6.4 Kronecker Delta Relations

The discrete Fourier transform relies on two Kronecker delta relations

$$\frac{1}{N} \sum_{p=0}^{N-1} e^{i2\pi(j-k)p/N} = \delta(j-k) \quad (1.11)$$

$$\frac{1}{N} \sum_{j=0}^{N-1} e^{i2\pi j(p-p')/N} = \delta(p-p') , \quad (1.12)$$

where  $j, k, p, p'$  are integers. To really understand these, consider the ‘pure’ claim

$$\frac{1}{N} \sum_{j=0}^{N-1} e^{i2\pi jp/N} = \delta(p) , \quad (1.13)$$

and expand out the sum manually:

$$\sum_{j=0}^{N-1} e^{i2\pi jp/N} = 1 + e^{i2\pi p/N} + e^{i2\pi 2p/N} + \cdots + e^{i2\pi(N-1)p/N}$$

In this form, the sum looks especially like a geometric series, which in general obeys

$$\frac{1-z^n}{1-z} = 1 + z + z^2 + \cdots + z^{n-1} ,$$

thus the above sum is

$$\sum_{j=0}^{N-1} e^{i2\pi jp/N} = \frac{1 - e^{i2\pi p}}{1 - e^{i2\pi p/N}} .$$

The above can only take one of two values. The interesting case is  $p = 0$ , leading to

$$\sum_{j=0}^{N-1} e^{i2\pi j0/N} = \sum_{j=0}^{N-1} 1 = N .$$

For *all* other integer values of  $p$ , the sum resolves to *zero*, as

$$1 - e^{i2\pi p} = 0 \quad p = 1, 2, 3, \dots .$$

In summary, we have found

$$\frac{1}{N} \sum_{j=0}^{N-1} e^{i2\pi jp/N} = \begin{cases} 1 & \text{if } p = 0 \\ 0 & \text{if } p \neq 0 \end{cases} ,$$

which is precisely (1.13). Note the argument  $p$  can be easily substituted and/or linearly shifted to recover (1.11)-(1.12).

## 6.5 Implementing the DFT

It's worth noting first that equations (1.1)-(1.2) apply for the continuum of times between each  $t_p$ , thus the more general equations read:

$$x(t) = \sum_{j=1}^{N \leq P} r_j \cos(\phi_i + \omega_j t) \quad (1.14)$$

$$y(t) = \sum_{j=1}^{N \leq P} r_j \sin(\phi_i + \omega_j t) \quad (1.15)$$

The star result of the DFT derivation is equation (1.10), namely

$$Q_j = \frac{1}{N} \sum_{p=0}^{N-1} z_p e^{-i2\pi j p / N}.$$

As pseudo-code, the implementation (1.10) looks like:

```
Function DFT (GivenPoint(), j0) {
    N = Size(arr)
    re = 0
    im = 0
    For k = 0 TO N - 1
        arg = 2 * Pi * k * j0 / N
        (u, v) = ComplexMult (COS(arg), SIN(arg),
                               GivenPoint(k).x, GivenPoint(k).y)
        re = re + u
        im = im - v
    Next k
    re = re / N
    im = im / N
    Return (re, im)
}
```

The array *GivenPoint()* refers to the list of  $P$  given points represented by  $z_p$ . The output of the *DFT* function is the  $j$ th pair of Fourier coefficients  $Q_j$ . Translating each  $Q_j$  back into radius and phase data is done as follows:

```
For j = 0 TO N - 1
    omega(j) = j
    If (j > N / 2) { omega(j) = j - N }
```

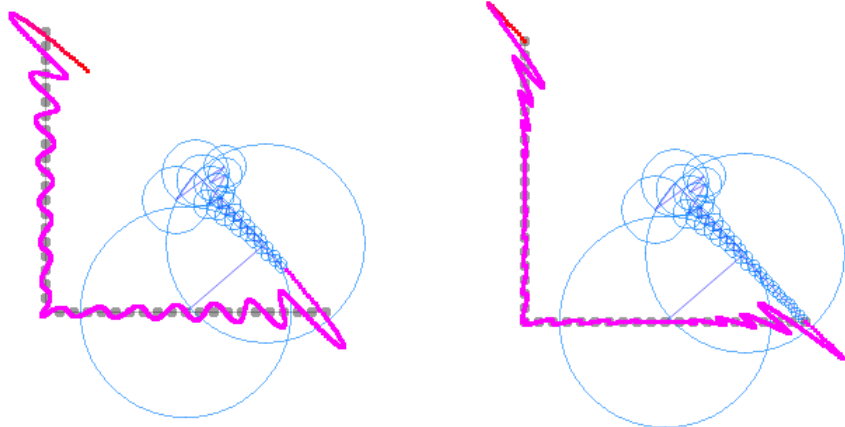


Figure 1.29: Approximation of open L-shape curve.  $N/P \approx 0.75$ .

Figure 1.30: Approximation of open L-shape curve.  $N = P$ .

```

(Q(j).x, Q(j).y) = DFT (GivenPoint(), j0)
rad(j) = Sqr(Q(j).x^2 + Q(j).y^2)
phase(j) = Atan2(Q(j).y, Q(j).x)
Next

```

---

## 6.6 Open Curves

More heavy-hitting issues are accessible now that we're in the big leagues. One interesting question is how *open* curves with many points  $P$  are approximated, particularly for mid-range  $N$ . Checking this out for an L-shaped curve, we see in Figs. 1.29-1.30 that the approximate curve does connect all given points, but the intermediate behavior near the boundaries is a bit ‘jumpy’.